Influence of grain size, organic carbon and organic matter residue content on the sorption of per- and polyfluoroalkyl substances in aqueous film forming foam contaminated soils - Implications for remediation using soil washing

Michel Hubert [a,b,*], Hans Peter H. Arp [a,b], Mona Cecilie Hansen [b], Gabriela Castro [a], Thomas Meyn [a], Alexandros G. Asimakopoulos [a], Sarah E. Hale [b]

[a] Norwegian University of Science and Technology (NTNU), NO-7491 Trondheim, Norway
[b] Norwegian Geotechnical Institute (NGI), NO-0806 Oslo, Norway

HIGHLIGHTS

- PFAS sorption analysed for different size fractions of an AFFF contaminated soil.
- First PFAS K_d & K_{oc} values for size fractions and soil organic matter residues.
- Residues showed the highest K_d values for PFAS sorption.
- In situ PFAS sorption significantly correlated with grain size and OC content.
- Recommendations for optimizing soil washing for PFAS presented.

GRAPHICAL ABSTRACT
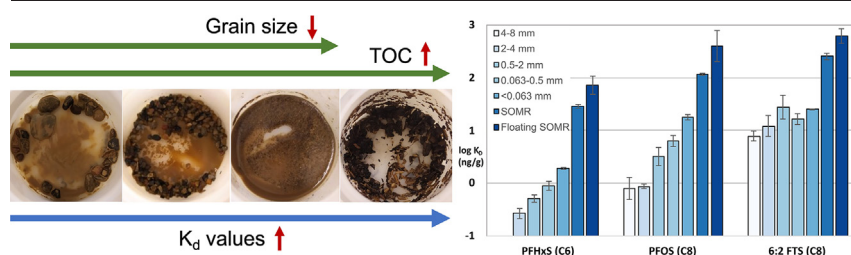
ARTICLE INFO

ABSTRACT

A soil that was historically contaminated with Aqueous Film Forming Foam (AFFF) was dry sieved into size fractions representative of those produced during soil washing. Batch sorption tests were then conducted to investigate the effect of soil parameters on in situ per- and polyfluoroalkyl substances (PFAS) sorption of these different size fractions: < 0.063 mm, 0.063 to 0.5 mm, 0.5 to 2 mm, 2 to 4 mm, 4 to 8 mm, and soil organic matter residues (SOMR). PFOS (513 ng/g), 6:2 FTS (132 ng/g) and PFHxS (58 ng/g) were the most dominant PFAS in the AFFF contaminated soil. Non-spiked, in situ K_d values for 19 PFAS ranged from 0.2 to 138 L/Kg (log K_d −0.8 to 2.14) for the bulk soil and were dependant on the head group and perfluorinated chain length (spanning C_4 to C_{13}). The K_d values increased with decreasing grain size and increasing organic carbon content (OC), which were correlated to each other. For example, the PFOS K_d value for silt and clay (< 0.063 mm, 17.1 L/Kg, log K_d 1.23) were approximately 30 times higher compared to the gravel fraction (4 to 8 mm, 0.6 L/Kg, log K_d −0.25). The highest PFOS K_d value (116.6 L/Kg, log K_d 2.07) was found for the SOMR fraction, which had the highest OC content. K_{oc} values for PFOS ranged from 6.9 L/Kg (log K_{oc} 0.84) for the gravel fraction to 1906 L/Kg (log K_{oc} 3.28) for the silt and clay, indicating that the mineral composition of the different size fractions also influenced sorption. The results here emphasize the need to separate coarse-grained fractions and fine-grained fractions, and in particular the SOMR, to optimize the soil washing process. Higher K_d values for the smaller size fractions indicate that coarser soils are better suited for soil washing.

1. Introduction

Aqueous film forming foams (AFFFs) have been used at firefighting training sites worldwide for decades (Anderson, 2021; Bräunig et al., 2019; Høisæter et al., 2019; Langberg et al., 2019; Sörengård et al., 2022). It is very common at airport sites that per- and polyfluoroalkyl

* Corresponding author at: Norwegian University of Science and Technology (NTNU), NO-7491 Trondheim, Norway.
E-mail address: Michel.Hubert@ngi.no (M. Hubert).

substances (PFAS) and related precursors accumulate in soil (Houtz et al., 2013; Maizel et al., 2021). The PFAS concentrations found at firefighting training sites where AFFF has been used are often orders of magnitude higher than those found in soils that are considered to represent background levels (Brusseau et al., 2020). These soils leach PFAS, and the development of hot spot groundwater plumes constitutes a large risk for the contamination of drinking water resources and aquatic ecosystems nearby (McMahon et al., 2022; Sörengård et al., 2022). PFAS emission are not limited to the usage of AFFF at airport or military bases. Other sources of PFAS include compost applications, the use of biosolids (Bolan et al., 2021a) and recycled water for irrigation purposes (O'Connor et al., 2022), landfill leachate (Gallen et al., 2017; Masoner et al., 2020) and emissions from industrial sites where PFAS are produced or used as processing aids (Kurwadkar et al., 2022). According to a recent publication, around 100,000 sites in Europe are potentially contaminated with PFAS, including firefighting training facilities at airports or military bases (Goldenman et al., 2019). Given the large number of PFAS impacted sites and stricter regulatory focus, which includes a drive to increase the amount of soil that can be reused, there is an ongoing need to develop diverse and innovative treatment technologies for PFAS contaminated soil (Bolan et al., 2021b; Ross et al., 2018).

A potential solution for some sites is soil washing. The main goal of soil washing is to transfer the contaminant into the liquid phase, where further treatment or concentration steps are easier to carry out (Quinnan et al., 2022). Soil washing generates much lower volumes of hazardous waste which need to be further treated or disposed of when compared to landfilling and stabilization. There are two different treatments regarding soil washing: in situ or ex situ. In an in situ approach, the soil is not excavated but is washed using enhanced irrigation, where the water is collected in a drainage system or through pumping wells. The effectiveness of in situ soil washing for an AFFF contaminated site was demonstrated at the pilot scale in Norway (Høisæter et al., 2021). The process of ex situ soil washing includes excavation followed by separation of different soil fractions using physical sieving techniques followed by a washing process. Depending on the type of soil and the predominated contaminants present, different physical and chemical techniques can be used in the process. To date there are few soil washing facilities in the world that are dedicated to the treatment of PFAS contaminated soils. The few previous publications reported examples at bench and field scales, both in situ and ex situ (Grimison et al., 2020; Høisæter et al., 2019; Quinnan et al., 2022). At a military base in Australia (RAAF Edinburgh) approximately 4,000 tons of PFAS contaminated soil were washed on site. Results demonstrated that around 90 % of PFOS and PFHxS were removed in clay soils and around 98 % were removed in sandy soils (Grimison et al., 2020). Quinnan et al. (2022) demonstrated the efficiency of soil washing using a pilot scale mobile washing treatment process at a remote airbase in Fairbanks, Alaska. In that trial approximately 180 tons of PFAS contaminated soil with maximum PFOS concentrations of 560 μg/kg were treated. The concentration of PFAS was reduced by approximately 95 % for the gravel fraction and by approximately 89 % for the sand fraction of the soil. The fine fraction (silt and clays) showed the lowest reduction (and greatest variance) of PFAS concentrations (approximately 62 %). These results indicated that the effect of washing may be related to soil grain size distribution and other soil properties, however, the influence of these properties is currently a knowledge gap. A better understanding of the soil parameters governing PFAS sorption will allow local pedological information to be used to screen soils for their suitability towards soil washing.

To address these knowledge gaps, this study focuses on understanding how different soil parameters affect PFAS sorption from historical AFFF contaminated soil and subsequently how this may affect the efficiency of a soil washing process. Several previous studies have shown that sorption processes are correlated with, among other parameters, the soil organic matter (SOM) content, the soil clay content as well as counter-ions present (Brusseau, 2018; Li et al., 2018; Milinovic et al., 2015; Nguyen et al., 2020). PFAS sorption interactions with organic matter (OM) are diverse and include hydrophobic interactions, electrostatic interactions and hydrogen bonding (Higgins and Richard, 2006; Li et al., 2018; Mei et al., 2021), whereas the sorption interactions of PFAS with soil minerals are dominated by electrostatic interactions (Campos-Pereira et al., 2020; Jeon et al., 2011; Mei et al., 2021). The specific surface area may play an important role in sorption especially for fine sized soil fractions, like clays, where cation exchange between PFAS and base cations covering the clay surface can occur (Mejia-Avendañ et al., 2020).

In this study the effect of selected soil parameters (organic carbon content, inorganic carbon content, percentage silt and clay, and specific surface area) of different soil size fractions (< 0.063 mm up to 8 mm) was investigated using batch tests with historical AFFF contaminated soil (Hale et al., 2017). The different soil size fractions are representative of those produced at different points in the soil washing process. The hypothesis of the experiments in this study are: PFAS sorption is dependent on a) grain sizes, b) OM content and c) chain-length. Testing of these hypotheses will support the optimization of soil washing as a remediation method for PFAS contaminated soil as well as contribute to our understanding of PFAS sorption mechanisms under saturated conditions.

2. Materials and methods

2.1. Soils and sieving procedure

Soil samples were collected from a historical AFFF contaminated site at Oslo airport, Gardermoen. The soil was taken between 0.1 and 0.5 m below the surface from the plant root zone (Fig. S1 of the Supplementary Material). Before further processing the soil was dried in an oven at 60 °C for 72 h. Aggregates formed during the drying process were gently crushed before sieving in order not to alter the derived size fractions. The soil was dry sieved following standard EN ISO 17892-4:2016 using a sieving tower with 8 different sieves (0.063, 0.125, 0.250, 0.500, 1.00, 2.00, 4.00, and 8.00 mm) (ISO, 2016). The sieving was stopped when there was no significant change in the mass of the size fractions on each sieve (mass difference after each sieving stage < 1 %).

For the size fractions up to 2 mm, hydrometer analysis following standard EN ISO 17892-4:2016 was conducted to calculate the remaining silt and clay content in the samples. A batch soil sample was made by mixing the sieved soil samples together in groups (<0.063 mm, 0.063 mm to 0.5 mm, 0.5 to 2 mm, 2 to 4 mm, 4 to 8 mm) to represent the soil fractions which are typically derived at soil washing plants. The different size fractions used in this study are shown in the Supplementary Material (Fig. S2). The composition of these fractions resembled the original sieve distribution of the soil.

2.2. Soil characterization

The different size fractions derived from the bulk soil were analysed for organic carbon (OC) and inorganic carbon (IC) content following an optimized loss on ignition method according to (Wang et al., 2011). Duplicate soil samples were dried at 105 °C over night (> 12 h) and then placed into the furnace at 475 °C, 550 °C and 800 °C. After each temperature step, the samples were quenched using a desiccator and weighed.

Specific surface area (SSA, [m^2/g]) was determined using the Brunauer-Emmet-Teller (N_2-BET) method (in duplicate). The samples were degassed at 105 °C for 12 h before being analysed using a Micromeritics 3FLEX 3500 instrument. Further soil characterization of the bulk soil can be found in (Hale et al., 2017).

2.3. Separation of soil organic matter residues

The soil contained soil organic matter residues, likely from plant roots, decayed organic material and plant residues. These organic residues (referred to as "SOMR" herein) were handpicked using metal tweezers from the sieve with a mesh size > 0.5 mm (Fig. S3). The amount of SOMR collected from these fractions are summarized in Table S1. Below this size

fewer SOMR were visible and it was difficult to both separate and distinguish these from the bulk soil.

2.4. Batch sorption experiments

To quantify in situ sorption of PFAS present on the different soil size fractions from historical contamination, single step batch tests were carried out based on a slightly modification of EN 12457-1 (EN, 2002). In short, triplicate batch tests were set up using 50 mL Falcon® conical centrifuge tubes at a normalized liquid (Milli-Q water containing 0.01 M CaCl$_2$) to solid ratio of 2:1 (apart from the SOMR at 30:1). Based on PFAS concentrations and soil properties, soil washing facilities adjust the amount of washing water, and hence the L:S ratio they use. In general L:S ratios are higher in soil washing facilities compared to this batch sorption study conducted under controlled laboratory conditions. For example, Grimison et al. (2023) used 18 m^3 per ton of soil for their field trial in Australia, leading to an effective L:S ratio of 18:1. To reach sorption equilibrium conditions between the water and solid phase, the vials were placed on an overhead shaker for 10 days (Hale et al., 2017; Higgins and Richard, 2006; Wang et al., 2021) followed by centrifugation (10 min, 3,200 rpm) and the removing of the supernatant water phase. Water and soil samples were stored at 4 °C prior to analysis.

When the water was added to the batches, some of the remaining SOMR in the soil floated on the water surface. These SOMR were collected after shaking and analysed as an additional fraction (referred to as "floating SOMR").

2.5. PFAS analysis

Water and soil samples were analysed for 40 PFAS in total. Information about all PFAS including CAS number, acronym, chemical structure, molecular weight, and the respective isotopically labelled internal standard used can be found in the Supplementary Material (Table S2). The analytical standards used in this study included PFAS in acid form and in salt form. The Instrumental LOQ and the method LOQ for water and soil can be found in Table S3. The OECD (2011) has defined short-chain perfluoroalkyl carboxylic acids (PFCAs) as those with a carbon chain length smaller than 8 ($< C_8$) and short-chain PFSAs with a carbon chaing length smaller than 6 ($< C_6$). Due to the sorption behaviour seen in this study we use the term "shorter" chain PFCAs to include all those with a carbon chain length of 8 or smaller ($\leq C_8$) and "shorter" chain PFSAs as having a carbon chain length of 7 or smaller ($\leq C_7$). PFCAs and PFSAs which are not included as shorter chain are referred to as "longer" chain.

The gravel size fraction (2 to 4 and 4 to 8 mm) was very heterogeneous and the mass balance for this fraction had a high error. For this reason, PFAS concentrations for the AFFF contaminated bulk soil (C_{bulk} [ng/g]) are calculated as the sum of concentrations found in the water (C_w [ng/mL]) and the soil phase (C_s [ng/g]) for each soil fraction used in the batch test.

2.6. Data analysis

Soil-water partitioning coefficients (K_d values) were calculated for each sample using the concentrations of PFAS measured in the soil phase (C_s [ng/g], d.w.) divided by those measured in the water phase (C_w [ng/mL]). K_d values were only calculated for samples where the PFAS concentration in the soil and the water were above the LOQ. Values below the LOQ were not substituted and were not used (Helsel, 2006). An average K_d was calculated using the single K_d values from each triplicate and the data is presented as the geometric mean ± standard error (± SE) (this would correspond to the arithmetic mean of log K_d values). K_{oc} [L/kg] values were calculated by normalizing K_d values with the organic carbon content and are presented as the geometric mean ± SE (OECD, 2001).

The K_d (and corresponding K_{oc}) values derived in this study are from sorption experiments, where historical AFFF contaminated soil was used.

A discussion on the comparability of K_d values from different studies can be found in Section 3.3.1.

2.7. Statistical analysis

Statistical analyses including the calculation of correlation coefficients and linear regression were carried out using IBM SPSS Statistics (28.0.1.0142). Collinearity between soil parameters was assessed using the calculated Pearson Correlation coefficients. In case of closely related soil properties (Pearson correlation coefficient, $r \geq 0.7$) (Nguyen et al., 2020) the soil property available for all size fractions and with the lowest error margin was chosen for the regression model. The mean grain size used in the regression model was calculated for each size fraction based on the results of the sieving analysis. The results of the regression models are compared using the adjusted R^2-values (adj. R^2) and calculated t-values for only significant models (p-value < 0.05).

2.8. Quality assurance and quality control (QA/QC)

QA/QC protocols were implemented during all experimental and analytical steps and a detailed description are provided in the Supplementary Material (S4). PFAS concentrations were quantified using matrix-match calibration described in studies before (Asimakopoulos et al., 2016; Castro et al., 2022; Raposo and Barceló, 2021). A detailed description of the sample preparation and analysis of PFAS can be found in the Supplementary Material (S3). To minimize losses of PFAS due to sorption to filter equipment (Lath et al., 2019; Sörengård et al., 2020) the water samples were not filtered. Sorption losses to vials as reported by various authors (Lath et al., 2019) were assumed to be negligible due to the high original concentrations of PFAS in the soil.

3. Results and discussion

3.1. Soil parameters

The soil was characterized as a medium sand (Fig. S6) with 85.2 % of material in the sand fraction (0.063 to 2.0 mm), 11.4 % in the silt and clay fractions and 3.2 % in the gravel fraction (2.0 to 8.0 mm). All measured soil parameters are summarized in Table S4. The handpicked SOMR (which are not included in the sand, silt, clay, or gravel fractions) represented around 0.2 % of the whole soil mass. The fine sand size fraction (0.063 to 0.5 mm) contained a considerable amount of silt (7.1 %) and clay (3.4 %), showing the limitation of the separation efficiency of the dry sieving technique for such small particles. The fraction < 0.063 mm mainly consisted of silt and had a smaller amount of clay (9.9 %). The results of the hydrometer analysis are summarized in Table S5.

Fig. 1 shows the results and errors of the N$_2$-BET analysis (SSA [m^2/g]) and the results of the enhanced loss on ignition method (for the determination of OC [%]) for the different size fractions used in the batch tests.

The OC content of the bulk soil was approximately 3.0 %. The OC content and the SSA both increase with decreasing grain size (Fig. 1). The fractions with the highest OC content were the silt-clay (< 0.063 mm) fraction (8 %) and the handpicked SOMR (44 %). The increase in OC content with decreasing soil aggregate size and soil size fraction resulted in the clay and silt fraction having the highest OC content and this is in accordance with various other studies (Anderson et al., 1981; Yang et al., 2016). As expected, the SSA of the gravel fraction (4 to 8 mm) was the smallest (1.47 m^2/g) and the silt-clay fraction (< 0.063 mm) had the highest SSA (4.58 m^2/g). Whereas the SSA for the sand fraction (0.063 to 2 mm) was nearly constant (0.5 to 2 mm = 2.88 m^2/g and 0.063 to 0.5 mm = 2.67 m^2/g). Compared to the silt-clay fraction, the SOMR had a lower and more variable SSA (2.51 m^2/g) and a substantially higher OC content. It is thus unique compared to the other grain-size fractions analysed. The larger errors for the SSA of the SOMR and the gravel fraction compared to the sand and silt fraction can be explained by the inherent heterogeneity of those samples.
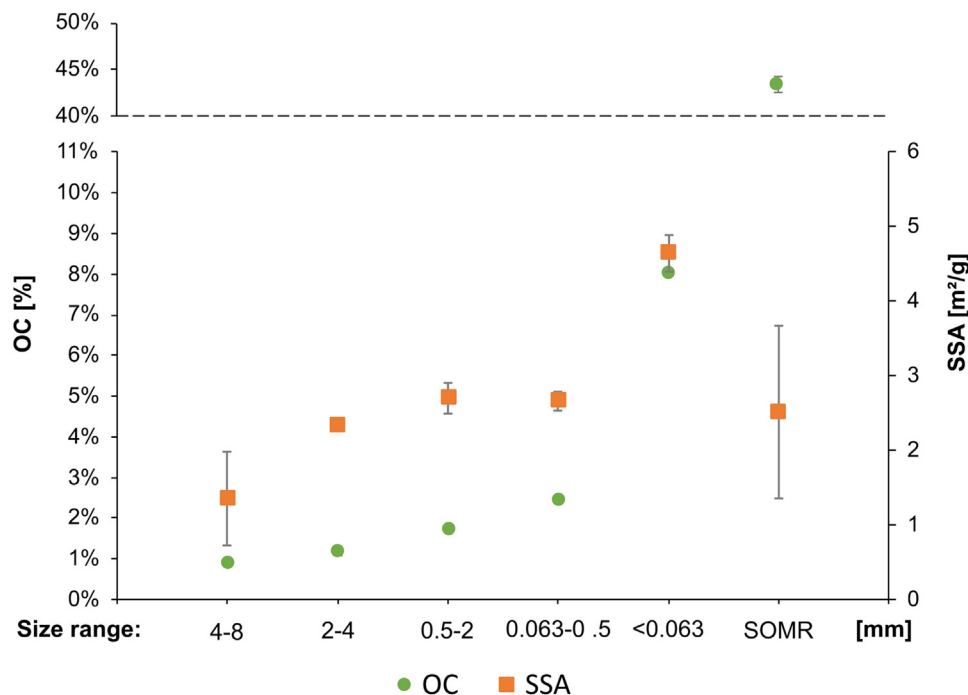
Fig. 1. Organic Carbon Content (OC) and Specific Surface Area (SSA) shown for each of the size fractions (mm).

The SSA of soil depends on both soil properties (e.g., OC content, mineral composition) and on the sample preparation methods used (e.g., degassing temperature and time) (Sokołowska, 2011). The SSAs measured in this study were in the same range as reported by other studies (Niskanen and Mänthylahti, 1988; Yukselen and Kaya, 2006). Studies by different authors found positive correlations between OC and SSA when they used the Ethylene Glycol Monoethyl Ether method and water vapor method to measure SSA (Arthur et al., 2023; De Jong, 1999). De Jong, 1999 could not confirm this positive correlation between OC and SSA, when the BET-N$_2$ method was used and even found a negative correlation between both soil parameters. An explanation for this trend is that soil organic matter may reduce the access of nitrogen molecules to the particle surfaces, due to coating and clogging of micro- and macropores (Kaiser et al., 1996; Pennell et al., 1995; Pignatello et al., 2006). This mechanism could explain the low SSA values for the SOMR with comparable high OC content found in this study.

3.2. PFAS concentration in soil

Nineteen out of the 40 analysed PFAS (Table S2), were detected at concentrations above 2 ng/g in the bulk soil and these PFAS are included in the subsequent discussion. These 19 PFAS (as PFAS$_{\Sigma19}$) make up 99.8 % of the total PFAS found in the bulk soil, which is equivalent to 858 ng/g (Table S6).

3.2.1. Bulk soil

In the bulk soil PFOS was the dominate PFAS and was detected at a concentration of 513 ng/g (60 % of the PFAS$_{\Sigma19}$), followed by 6:2 FTS (132 ng/g, 15 % of the PFAS$_{\Sigma19}$), PFHxS (58 ng/g, 7 % of the PFAS$_{\Sigma19}$) and FOSA (35 ng/g, 4 % of the PFAS$_{\Sigma19}$). The concentration of the other 15 PFAS in the bulk soil were between 24 ng/g (PFHxA) and 3 ng/g (10:2 FTS) (contributing between 3 and 0.4 % of the PFAS$_{\Sigma19}$, respectively). The PFAS concentrations and distributions in the bulk soil are in the same range as those found at other highly contaminated sites. At the airport site in this study, AFFF containing PFOS was used from 1989, and when PFOS was restricted in Europe in 2009 (The Commission of the European Communities, 2009), it was replaced with an AFFF product dominated by 6:2 FTS (Høisæter et al., 2015). Different field studies from various airports in several

countries have reported PFOS and 6:2 FTS as the most abundant PFAS in AFFF contaminated soil, where different chemical formulations of AFFF have been used (Baduel et al., 2015; Bräunig et al., 2019; Hale et al., 2017; Langberg et al., 2019; Maizel et al., 2021; Nickerson et al., 2020). These studies have also reported lower concentrations of PFCAs and PFAS precursors such as Perfluorooctanesulfonamide (FOSA) in AFFF contaminated soils.

Hale et al. (2017) previously studied the same AFFF contaminated area and found PFOS (6.4 to 2,400 ng/g) and 6:2 FTS (13 to 92.4 ng/g) to be the two most abundant PFAS in soil samples taken from 21 different locations and several different depths. Lower concentrations were found for PFPeA (2.8 ng/g), PFHxS (3.0 to 25.3 ng/g), PFNA (2.8 to 41.3 ng/g), PFDA (2.6 to 72.1 ng/g), 8:2 FTS (3.8 to 116 ng/g) and PFOA (3.0 to 13.0 ng/g). Baduel et al. (2015) analysed 15 soil samples (spatially distributed) taken from a firefighting training pit where an AFFF was used until 2010 before transitioning to a fluorine free foam. The study screened for in total 11 PFCAs, 4 PFSAs and 6:2 FTS. The authors found PFOS (resembling 83 % of total mean PFAS, ranging from 79 to 223,983 ng/g) and PFHxS (3 % of total mean PFAS, 115 to 4,391 ng/g) to be the two most abundant PFAS in the soil. Both compounds have been found in the surface soil layer in all sample locations. Lower concentrations were found for other PFCAs (PFPeA, PFHxA, PFHpA, PFOA, PFNA, PFUnA, PFTriDA) and PFSAs (PFBS, PFDS) in this study. Houtz et al. (2013) investigated soil and water samples from an AFFF contaminated site reported that PFOS accounted for approximately 77 % of the total PFAS content in the soil, fluorotelomer based precursors (such as 6:2 FTS and 8:2 FTS) accounted for approximately 10 % and the sulfonamide based PFAA precursors (including FOSA) accounted for approximately 5 % of the total PFAS in the soil.

3.2.2. PFAS$_{\Sigma19}$ in different soil size fractions

Fig. 2 shows the distribution of PFAS$_{\Sigma19}$ for the bulk soil and the different size fractions. The bulk soil and all size fractions are dominated by PFOS and 6:2 FTS, which together made up for 56.6 % (4 to 8 mm) to 78.5 % (SOMR) of the PFAS$_{\Sigma19}$ concentration. Overall PFOS is the most abundant PFAS in all size fractions, ranging from 50.7 % (4 to 8 mm) up to 69.3 % of the PFAS$_{\Sigma19}$ (2 to 4 mm).

The relative distribution of PFAS$_{\Sigma19}$ on the different grain size fraction in the bulk soil sample is presented in Table 1. PFAS$_{\Sigma19}$ concentrations
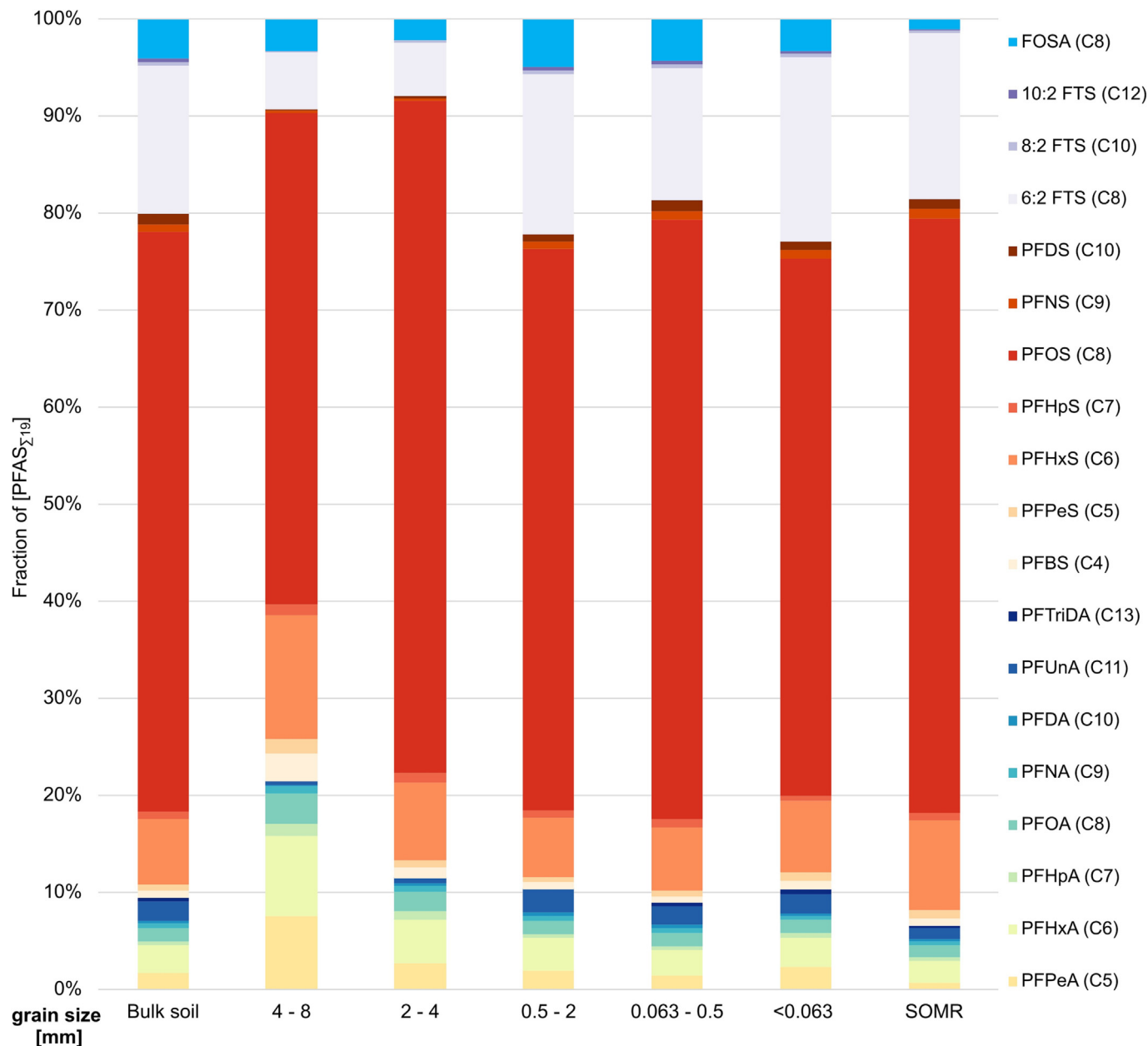
Fig. 2. Concentration of PFAS$_{\Sigma 19}$ for the bulk soil and the different size fractions.

decreased with increasing size fraction. The concentrations ranged from 1,855 ng/g for the silt and clay fraction (< 0.063 mm) down to 54 ng/g for the gravel size fraction (4 to 8 mm). The SOMR had the highest PFAS$_{\Sigma 19}$ concentrations of 5,259 ng/g.

Table 1
PFAS$_{\Sigma 19}$ in the bulk soil and the soil grain size fractions.

Soil grain size	PFAS$_{\Sigma 19}$ [ng/g size fraction]	PFAS$_{\Sigma 19}$ [ng/g bulk soil]	PFAS$_{\Sigma 19}$ in each size fraction [wt%][a]
4 to 8 mm	53.5	0.9	0.1
2 to 4 mm	152.5	2.4	0.3
0.5 to 2 mm	421.9	98.2	11.4
0.063 to 0.5 mm	863.2	534.3	62.3
< 0.063 mm	1,854.7	212.5	24.7
SOMR	5,258.6	10.0	1.2
Sum		858.2	100

[a] Values are calculated by dividing PFAS$_{\Sigma 19}$ concentration in each size fraction [ng/g] by the total PFAS$_{\Sigma 19}$ concentration in the bulk soil [858.2 ng/g].

Table S7 summarize the C_{Bulk} for PFAS$_{\Sigma 19}$ (including SE) for each size fraction. For PFOS, the C_{Bulk} detected in the smallest size fraction (< 0.063 mm, 1,027 ng/g) was approximately 40 times higher than for the gravel size fraction (4 to 8 mm, 27 ng/g). For 6:2 FTS, the C_{bulk} in the smallest size fraction < 0.063 mm (352 ng/g) was approximately 100 times higher than the gravel size fraction (4 to 8 mm, 3.2 ng/g). A similar trend can be seen for PFOA where the C_{bulk} is approximately 15 times higher for the silt and clay fraction (25 ng/g) compared to the gravel fraction (4 to 8 mm, 1.6 ng/g).

Table 1 presents the proportion each size fraction contributed to the total PFAS$_{\Sigma 19}$ [% and ng/g bulk soil]. The PFAS$_{\Sigma 19}$ in the gravel fraction (4 to 8 mm) only represented 0.1 % of the PFAS$_{\Sigma 19}$ mass in the soil, which means that this fraction could lend itself to being washed and then reused most easily. The largest mass of PFAS$_{\Sigma 19}$ is found in the fine sand fraction (0.063 to 0.5 mm). Overall 62.3 % (534 ng/g bulk soil) of PFAS$_{\Sigma 19}$ is associated with this fraction, while the PFAS$_{\Sigma 19}$ concentration in the silt and clay fraction (< 0.063 mm) accounted for 24.7 % (213 ng/g bulk soil). The results presented here highlight the importance of

understanding the sorption mechanisms at play for the different size fractions as these will affect the efficiency of the soil washing process, as will be discussed further below.

3.3. Partition coefficients (K_d values)

3.3.1. Bulk soil

The experimental K_d values and standard errors ($\pm$ SE) for the bulk soil, based on the different size fractions, for all cases where PFAS were present in the soil and water sample above the LOQ, are presented in Table 2.

Hale et al. (2017) used the same soil, though sampled from a different location and reported a K_d value for PFOS of 8.8 L/kg which is similar to the mean value found in this study (6.5 L/kg). Høisæter and Breedveld (2022) carried out column experiments using the same soil as in the study here to investigate the leaching potential of the soil. In their study, K_d values were calculated at assumed equilibrium (L/S = 0.1 and following stagnant conditions for 3 days) and the values reported were in a similar range for most of the PFAS considered here. Nguyen et al. (2020) carried out batch tests with 10 different soils (air dried and sieved with a 0.5 mm mesh) spiked with 29 PFAS. The OC content of two soils (S8 and S4), which are most similar to the one tested in this study varied from 0.75 to 2.64 % and the silt and clay content were between 6 and 54 %. These K_d values (at soil pH) are lower than in this study, 3.22 and 4.18 for PFOS, respectively, i.e. a factor of 2 lower (Table S8). A detailed comparison between the K_d values derived in this study and reported in the literature can be found in the Supplementary Material (Table S8).

Differences in reported K_d values can have multiple explanations. PFAS show nonlinear sorption isotherms and clear sorption dependency on soil parameters (Barzen-Hanson et al., 2017), which make the comparison between K_d values from different studies difficult. Overall K_d values derived from field samples, i.e. in situ K_d values, are consistently larger than from spiked laboratory studies (Li et al., 2018). This is consistent with the in situ K_d values found in this study compared to spiked studies, such as the one conducted by Nguyen et al. (2020). PFAS exhibit soil adsorption and desorption hysteresis based on their chemical structure and soil characteristics in play (Kookana et al., 2022; Xiao et al., 2019). Furthermore Schaefer et al. (2021) witnessed in their batch tests with AFFF contaminated soil, that short-chain PFAS tend not to reach equilibrium conditions even after 400 h of shaking time. The lack of equilibrium was attributed to slow diffusion-based desorption processes for these compounds. A study by Zhu et al. (2021) found that some PFAS can form non extractable residues, due to strong covalent binding (and possibly ligand exchange) as well as physical entrapment in meso- or macropores. The ongoing formation of these residues was reported in a study with a duration of 240 days, which is far longer than the duration of most spiked PFAS studies (Higgins and Richard, 2006; Nguyen et al., 2020). In addition to PFAS, soil from firefighting training sites often exhibit elevated levels of other co-contaminates like hydrocarbons and other surfactants, which will alter the sorption behaviour of PFAS (Høisæter and Breedveld, 2022). In conclusion, all these processes will lead to different K_d values based on the history of contamination and the experimental design of each study. The in situ K_d values obtained in this study provide a more accurate representation of the soil washing process compared to spike studies, which typically addresses historical soil contamination, including but not limited to PFAS contamination.

3.3.2. Effect of PFAS functional group on K_d value

Higher K_d values were determined for PFSAs compared to PFCAs with the same perfluorinated carbon chain length indicating stronger sorption to the soil. This is clearly visible for PFSAs with a chain length > C_7 (Table 2). For a perfluorinated chain length of C_8, the K_d values increased in the following order: PFCAs < PFSAs < FTS < FOSA. The higher sorption of PFSAs compared to PFCAs has been reported by various authors and can be explained by stronger interactions of the sulfonated headgroup compared to the carboxylic headgroup with the soil surface (Higgins and Richard, 2006; Li et al., 2018; Milinovic et al., 2015; Nguyen et al., 2020; Zareitalabad et al., 2013). Rodowa et al. (2020) conducted column experiments with AFFF contaminated groundwater using granular activated carbon to study sorption behaviour. The retardation of PFAS with the same perfluorinated carbon chain length increased in the order PFCAs < PFSAs < FTS < FOSA and corresponds with the increase of K_d values in this study. There is very little data comparing telomeric headgroups to perfluorinated headgroups; however, modelled K_{oc} values for the neutral telomer C_8 alcohol 6:2 FTOH telomer (CASRN 647–42-7) are lower compared to the perfluorinated C_8 alcohol pentafluorooctanol (CASRN 307–30-2), indicating telomeric alcohol headgroups should have a lower K_{oc} than perfluoralkylated alcohol headgroups (Table S9). The larger sorption of the anionic 6:2 FTS than the anionic PFOS indicates that the electron withdrawing effect of the neighbouring fluorines on the sulfonate headgroup on PFOS may cause the sulfonate on PFOS to have a stronger anionic charge than 6:2 FTS, increasing solubility and lowering K_d. Of all the C_8 PFAS investigated here (PFOS, PFOA, 6:2 FTS and FOSA), FOSA showed the highest K_d value (65.8 L/kg, Table 2), probably because at an environmentally relevant pK_a value of approximately 6.2 (Rayne and Forest, 2009), the head group becomes partially neutral which decreases water solubility and reduces electrostatic repulsion with the mostly negatively charged soil surface and thus leading to enhanced sorption (Nguyen et al., 2020; Rayne and Forest, 2009).

3.3.3. Effect of PFAS chain length on K_d value

K_d values for shorter chain PFCAs ($\leq C_8$) were similar ranging from 0.15 to 1.20 L/kg (log −0.83 to log 0.08) for the bulk soil (Table 2). For PFSAs ($\leq C_7$) the K_d values varied between 0.35 and 1.08 L/kg (log −0.46 to log 0.03). The effect of chain length on K_d values for the PFCAs and PFSAs was previously reported by Høisæter and Breedveld (2022) using samples from the same site. Nguyen et al. (2020) suggested that sorption of shorter chain PFAS to soil is mainly driven by electrostatic interaction of ionic groups with soil particles, rather than hydrophobic bonding (chain length dependant). For the longer PFCAs, the longer PFSAs and the FTS considered in this study, there was a significant

Table 2
Experimental K_d values (geometric mean $\pm$ SE) for the bulk soil (PFAS$_{\Sigma 19}$).

[C]	PFCAs	log K_d [L/kg]	K_d [L/kg]	PFSAs	log K_d [L/kg]	K_d [L/kg]	FTS and FOSA	log K_d [L/kg]	K_d [L/kg]
4				PFBS	−0.46 $\pm$ 0.02	0.35 $\pm$ 0.02			
5	PFPeA	−0.83 $\pm$ 0.02	0.15 $\pm$ 0.01	PFPeS	−0.46 $\pm$ 0.04	0.35 $\pm$ 0.03			
6	PFHxA	0.004 $\pm$ 0.02	1.01 $\pm$ 0.04	PFHxS	−0.04 $\pm$ 0.06	0.91 $\pm$ 0.13			
7	PFHpA	−0.12 $\pm$ 0.06	0.75 $\pm$ 0.11	PFHpS	0.03 $\pm$ 0.08	1.08 $\pm$ 0.20			
8	PFOA	0.08 $\pm$ 0.05	1.20 $\pm$ 0.15	PFOS	0.81 $\pm$ 0.08	6.51 $\pm$ 1.12	6:2 FTS	1.26 $\pm$ 0.11	18.08 $\pm$ 5.16
							FOSA	1.82 $\pm$ 0.14	65.84 $\pm$ 18.91
9	PFNA	0.39 $\pm$ 0.11	2.47 $\pm$ 0.67	PFNS	1.49 $\pm$ 0.06	31.14 $\pm$ 4.84			
10	PFDA	1.34 $\pm$ 0.09	21.98 $\pm$ 4.89	PFDS	2.02 $\pm$ 0.08	104.13 $\pm$ 22.47	8:2 FTS	1.47 $\pm$ 0.08	29.81 $\pm$ 6.19
11	PFUnA	2.14 $\pm$ 0.17	138.12 $\pm$ 74.42						
12							10:2 FTS	1.85 $\pm$ 0.29	70.46 $\pm$ 90.83
13	PFTriDA	1.40 $\pm$ 0.24	25.21 $\pm$ 19.66						

increasement in the K_d value with the chain length. The log K_d value increased linearly by 0.88 for PFCAs, by 0.66 for PFSAs and by 0.15 for FTS for each -CF_2 moiety (Fig. S7). Similar tendency has been reported previously (Higgins and Richard, 2006; Nguyen et al., 2020) and has been explained by the higher hydrophobicity, as chain length increases (Barzen-Hanson et al., 2017; Nguyen et al., 2020). It should be noted that PFTriDA (C_{13}) is not following this trend showing a smaller K_d value compared to the shorter PFUnA (C_{10}).

3.3.4. Effect of soil size fraction on K_d values

The mean, experimental log K_d values ($\pm$ SE) for each soil size fraction are summarized in Table 3.

According to the obtained results, log K_d value and size fraction (except for the SOMR) are inversely correlated, with the largest size fraction having the smallest log K_d. This is also the size fraction with the lowest OC and silt and clay content in this study (Fig. 1). In the case of PFNA (C_9), the lowest log K_d values (< LOQ to 0.07) were found for the gravel fractions (2 to 4 and 4 to 8 mm) and they increased for the sand fractions (0.063 to 0.5 and 0.5 to 2 mm) to values of 0.28 and 0.34. A similar trend can be seen for PFOS, where the log K_d values were $-$ 0.25 (4 to 8 mm) and $-$ 0.07 (2 to 4 mm) for the gravel size fractions, increasing to 0.40 (0.5 to 2 mm) and 0.76 (0.063 to 0.5 mm) for the sand fractions. They increased further for the silt and clay fraction (< 0.063 mm) where log K_d was 1.23, for the SOMR log K_d was 2.07 and the highest log K_d value was calculated for the floating SOMR (2.40 and 2.27 for PFOS and PFNA, respectively). This trend indicates that an increase in K_d value for some PFAS can be linked to soil parameters as OC content, which is decreasing with grain size (Section 3.1).

To the best of the authors knowledge, there are no previous studies where K_d has been calculated for PFAS for different soil size fractions. However, sieving is an often-used soil preparation technique (Milinovic et al., 2015; Nguyen et al., 2020; Nickerson et al., 2020; Umeh et al., 2021) and

as such reported K_d data is most often for soils that contain the finer and not the coarser grains (e.g., gravel fraction, coarse sand fraction). As a comparison for finer grained soils, (Milinovic et al., 2015) determined K_d values for PFOS, PFOA and PFBS for six different soils with varying textures (different sand and clay content) and OC contents (0.2 to 39 %). All soils were taken from the top layer of natural or agricultural habitats. The reported log K_d values ranged from 1.28 to 2.47 for PFOS, from 0.34 to 1.58 for PFOA and from -0.40 to 0.83 for PFBS. The highest K_d values were found in a peat soil (OC content = 39 %). The reported K_d values are in the same range as the K_d values reported for the sand, silt, and clay fraction and SOMR in this study. The K_d value for the floating SOMR were between 0.5 and 1 log unit larger than for the SOMR manually removed from the dry soil. For some of the shorter chain PFAS this increase was smaller (PFBS, PFPeS, PFHxA).

K_{oc} values were obtained by normalizing K_d values to the fraction of OC in the grain size samples (Table 4). The log K_{oc} values for the different PFAS ranged from 0.93 (PFHpA) to 4.01 (PFTriDA) for PFCAs, between 0.84 (PFOS) to 4.04 (PFDS) for PFSAs and between 1.96 (6:2 FTS) to 4.60 (10:2 FTS) for the FTS compounds. K_{oc} values for the bulk soil showed the same sorption trends regarding chain length and functional group dependency. As for K_d, K_{oc} values were inversely correlated with size fraction and the highest K_{oc} values were found for the silt and clay fraction (< 0.063 mm) for most PFAS. For PFOS, the lowest log K_{oc} values were found for the gravel fraction (4 to 8 mm, log 0.84 L/kg), and they increased by a factor of approximately 4 (log 3.28 L/kg) for the silt and clay fraction (< 0.063 mm). The in situ K_{oc} values for the different size fractions in this study are in the same range as the values compiled in the literature (Table 4), for both spiked (Campos Pereira et al., 2018) and historical contaminated soils (Høisæter and Breedveld, 2022). Exceptions are the gravel size fractions (2 to 4 and 4 to 8 mm) and the coarse sand fraction (0.5 to 2 mm) which have lower K_{oc} values for some PFAS, such as PFOS.

Table 3

Mean log K_d values for each of the PFAS$_{19}$ according to size fraction. Hatched cells indicate PFAS concentration < LOQ in soil and corresponding water samples for all three triplicates. (*) indicates triplicate samples where PFAS concentrations were < LOQ in two of the triplicates.

|	4-8 mm	2-4 mm	0.5-2 mm	0.063-0.5 mm	<0.063 mm	SOMR	Floating SOMR
PFPeA (C5)					0.11 ±0.02		1.79*
PFHxA (C6)		0.09 ±0.21	0.06 ±0.03	-0.08 ±0.02	0.18 ±0.01	1.27 ±0.03	1.61 ±0.03
PFHpA (C7)		0.21*	-0.84 ±0.18	-0.11 ±0.06	0.27 ±0.07	0.99 ±0.05	1.51 ±0.18
PFOA (C8)		0.02 ±0.18	-0.36 ±0.11	0.04 ±0.07	0.47 ±0.02	1.46 ±0.03	2.09 ±0.04
PFNA (C9)	0.07*		0.34 ±0.21	0.28 ±0.15	0.84 ±0.03	1.64 ±0.03	2.27 ±0.09
PFDA (C10)		0.74*	0.85 ±0.12	1.37 ±0.12	1.54 ±0.07	2.66 ±0.13	3.47 ±0.08
PFUnA (C11)			1.66 ±0.10	2.24 ±0.21	1.83 ±0.10	2.82 ±0.03	3.38 ±0.25
PFTriDA (C13)			1.72*	2.09*	1.90 ±0.05	2.43 ±0.12	2.95 ±0.33
PFBS (C4)			-0.43 ±0.02	-0.45 ±0.03	-0.34 ±0.02	1.00 ±0.06	1.40 ±0.09
PFPeS (C5)			-0.23*	-0.49 ±0.07	-0.23 ±0.02	1.12 ±0.05	1.20 ±0.20
PFHxS (C6)		-0.61 ±0.09	-0.31 ±0.06	-0.09 ±0.09	0.27 ±0.02	1.44 ±0.03	1.76 ±0.18
PFHpS (C7)			-0.35 ±0.11	-0.07 ±0.11	0.52 ±0.06	1.46*	1.94 ±0.19
PFOS (C8)	-0.25 ±0.21	-0.07 ±0.04	0.40 ±0.17	0.76 ±0.10	1.23 ±0.05	2.07 ±0.02	2.40 ±0.29
PFNS (C9)		0.71*	1.12 ±0.04	1.55 ±0.09	1.61 ±0.06	2.64 ±0.07	3.21 ±0.20
PFDS (C10)		0.94 ±0.17	1.69 ±0.06	2.12 ±0.11	1.76 ±0.06	2.83 ±0.09	3.39 ±0.17
6:2 FTS (C8)	0.86 ±0.10	0.95 ±0.20	1.25 ±0.22	1.17 ±0.10	1.40 ±0.01	2.38 ±0.07	2.73 ±0.14
8:2 FTS (C10)	0.73 ±0.18	0.44 ±0.22	1.13 ±0.03	1.53 ±0.11	1.62 ±0.03	2.18 ±0.08	3.08 ±0.13
10:2 FTS (C12)		1.48*	1.99 ±0.20	2.68*	2.32 ±0.01	2.55 ±0.06	2.98 ±0.18
FOSA (C8)	-0.13 ±0.26	0.38 ±0.14	1.44 ±0.09	1.92 ±0.15	1.73 ±0.09	2.65 ±0.16	3.54 ±0.06

log   -0.84   1.40   3.54
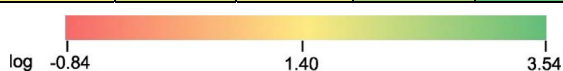
Table 4

Mean log K_{oc} values for each of the $PFAS_{19}$ according to size fraction. [a] values taken from (Campos Pereira et al., 2018) and [b] from (Høisæter and Breedveld, 2022), na = not available. Hatched cells indicate PFAS concentration < LOQ in soil and corresponding water samples for all three triplicates.

	4-8 mm	2-4 mm	0.5-2 mm	0.063-0.5 mm	<0.063 mm	SOMR	Floating SOMR	Values from other studies
PFPeA (C5)					2.16 ±0.02		2.15*	1.37[a]
PFHxA (C6)		1.70 ±0.21	1.83 ±0.03	1.84 ±0.02	2.23 ±0.01	1.63 ±0.03	1.97 ±0.03	1.31, 2.1[a]
PFHpA (C7)		1.83*	0.93 ±0.18	1.82 ±0.06	2.32 ±0.07	1.36 ±0.05	1.87 ±0.18	1.63, 2.1[a]
PFOA (C8)		1.63 ±0.18	1.41 ±0.11	1.96 ±0.07	2.52 ±0.02	1.82 ±0.03	2.45 ±0.04	1.89 to 3.5[a]
PFNA (C9)	1.17*		2.11 ±0.21	2.21 ±0.15	2.89 ±0.03	2.00 ±0.03	2.63 ±0.09	2.36 to 4.0[a]
PFDA (C10)		2.35*	2.62 ±0.12	3.29 ±0.12	3.59 ±0.07	3.02 ±0.13	3.83 ±0.08	2.96 to 4.6[a]
PFUnA (C11)			3.43 ±0.10	4.16 ±0.21	3.88 ±0.10	3.18 ±0.03	3.74 ±0.25	3.3 to 5.1[a]
PFTriDA (C13)			3.49*	4.01*	3.95 ±0.05	2.79 ±0.12	3.31 ±0.33	
PFBS (C4)			1.34 ±0.02	1.47 ±0.03	1.71 ±0.02	1.36 ±0.06	1.76 ±0.09	1.22, 1.79[a]
PFPeS (C5)			1.54*	1.44 ±0.07	1.82 ±0.02	1.48 ±0.05	1.56 ±0.20	na
PFHxS (C6)		1.00 ±0.09	1.46 ±0.06	1.84 ±0.09	2.32 ±0.02	1.80 ±0.03	2.12 ±0.18	2.05 to 3.7[a]
PFHpS (C7)			1.42 ±0.11	1.85 ±0.11	2.57 ±0.06	1.83*	2.3 ±0.19	na
PFOS (C8)	0.84 ±0.21	1.54 ±0.04	2.17 ±0.17	2.69 ±0.10	3.28 ±0.05	2.43 ±0.02	2.77 ±0.29	2.6 to 3.8[a]
PFNS (C9)		2.32*	2.89 ±0.04	3.47 ±0.09	3.66 ±0.06	3.00 ±0.07	3.57 ±0.20	na
PFDS (C10)		2.55 ±0.17	3.46 ±0.06	4.04 ±0.11	3.81 ±0.06	3.19 ±0.09	3.75 ±0.17	na
6:2 FTS (C8)	1.96 ±0.10	2.56 ±0.20	3.02 ±0.22	3.09 ±0.10	3.45 ±0.01	2.75 ±0.07	3.09 ±0.14	1.5 to 2.1[b]
8:2 FTS (C10)	1.82 ±0.18	2.05 ±0.22	2.89 ±0.03	3.45 ±0.11	3.67 ±0.03	2.55 ±0.08	3.45 ±0.13	3.1 to 3.6[b]
10:2 FTS (C12)		3.10*	3.76 ±0.20	4.60*	4.37 ±0.01	2.91 ±0.06	3.34 ±0.18	na
FOSA (C8)	0.97 ±0.26	1.99 ±0.14	3.21 ±0.09	3.84 ±0.15	3.78 ±0.09	3.01 ±0.16	3.90 ±0.06	4.2 – 4.5[a]

log   0.84   2.52   4.60
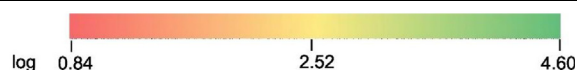
Unlike K_d, the log K_{oc} values for the longer chain PFCAs and PFSAs for the SOMR are in a similar range as the fine and coarse sand fraction (0.063 to 2 mm). The difference of K_{oc} and K_d between size fractions for selected PFAS are summarized in Table S10. The changes between the size fractions (except for the SOMR) are higher for K_{oc} than for K_d values. On the assumption that the nature and quality of OC found in the different size fractions is similar due to its common origin, the differences in K_{oc} values and the stronger increase between size fractions compared to the derived K_d values, indicate that other soil parameters (e.g mineral composition) besides OC, influence PFAS sorption behaviour.

3.4. Effect of soil properties on sorption

Previous studies (Barzen-Hanson et al., 2017; Huang et al., 2022) have shown that the interaction between PFAS and soils are complex and can be governed by multiple soil properties and environmental conditions. To statistically evaluate the effect of soil parameters (OC content, mean grain size, SSA, silt content and clay content) on PFAS sorption for the different size fractions in this work, single linear regression (SLR) was conducted for K_d and K_{oc} values. The results for SLR correlating each of the log soil parameters (SSA, silt and clay content, OC, IC, and mean grain size) with log K_d (Table S13 and Table S14) and log K_{oc} values (Table S15) are presented in the supplementary material. When all soil fractions are included, the SSA parameter is non-linear distributed. The other soil parameters used in the linear regression were seen to strongly correlate with each other. All calculated Pearson Correlation coefficients (PC) for all soil parameters can be found in the Supplementary Material (Table S11 and Table S12). OC content correlated (*p*-value < 0.01) with grain size (Pearson Correlation (PC) = −0.978), IC (PC = 0.872), silt (PC = 0.997) and clay content (PC = 0.974). Because OC was available for all size fractions, it was selected as the independent parameter for the single linear regression with K_d as dependant variable. The results of the SLR showed a positive correlation between OC and K_d values (Fig. 3), which is in accordance with other

studies and supports the hypothesis that the main driving force for PFAS sorption is favourable interactions of the PFAS with the OC (Campos Pereira et al., 2018; Higgins and Richard, 2006; Nguyen et al., 2020) compared to minerals or water.

A higher adjusted R^2-value and a higher t-value indicate a stronger correlation and therefore stronger dependency between K_d and OC. For the PFCAs, the adjusted R^2-values ranged from 0.52 (PFTriDA) up to 0.89 (PFOA) and corresponding t-values ranged from 3.0 (PFTriDa) to 10.1 (PFOA). For the PFSAs, the adjusted R^2-values ranged from 0.61 (PFDS) up to 0.96 (PFHxS and PFHpS) and correspond t-values ranged from 4.7 (PFDS) up to 17.5 (PFHxS). For the FTS compounds the adjusted R^2-values ranged from 0.37 (10:2 FTS) up to 0.75 (6:2 FTS) with t-values ranging from 2.5 (10:2 FTS) to 7.2 (6:2 FTS). These results indicate that the effect of OC on K_d value varied for different PFAS groups and carbon chain lengths. The higher adjusted R^2-values and t-values for PFSAs compared to PFCAs demonstrates the stronger correlation between K_d and OC for PFSAs (Fig. 3). Other studies have also reported that K_d values for PFSAs show a stronger correlation to OC than PFCAs (Ahrens et al., 2010; Campos Pereira et al., 2018; Zhang et al., 2013), indicating the sulfonate group may be exhibit a greater affiliation with organic carbon. The FTS compounds and FOSA showed a weaker correlation between K_d and OC compared to the PFCAs and the PFSAs, which may indicate an even weaker affiliation for these head groups with organic carbon (adj. R^2: 0.37–0.75), this was observed in other studies with soil before (Barzen-Hanson et al., 2017; Nguyen et al., 2020). Trends in the correlation of sorption to grain size/OC with chain-length were also evident. PFUnA (C_{11}) had a lower adjusted R^2-value (0.45) and t-value (3.2) compared to PFDA (C_{10}, 0.87, respectively 8.9). A similar trend can be seen for the PFSAs where the adjusted R^2-values and t-values peak at a chain length of C_6 (0.96, 17.5) and then decrease (PFDS, C_{10}, adjusted R^2-value 0.61, t-value 4.7). The adjusted R^2-values calculated for the FTS compounds decrease with chain length, with the lowest R^2-value of 0.37 for 10:2 FTS. Nguyen et al. (2020) reported similar findings as they also carried out a single linear
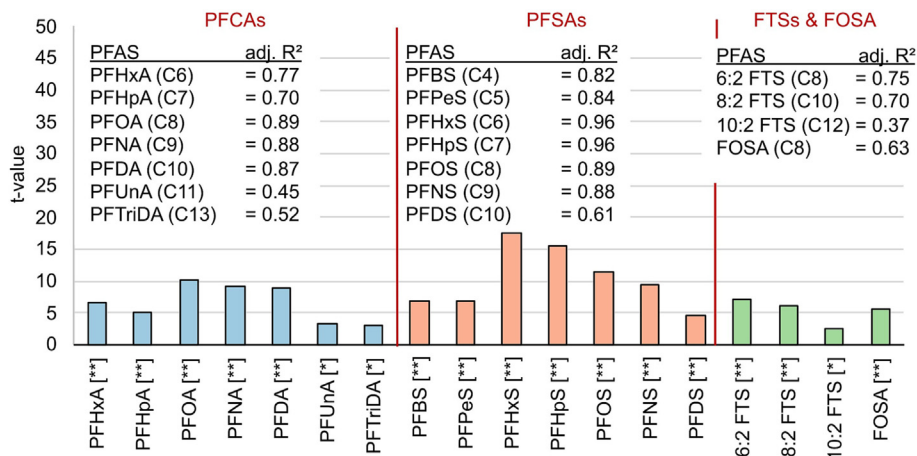
Fig. 3. Adjusted determination coefficients (adj. R^2) and t-values for the SLR model describing the regression of in situ K_d values with OC for PFASΣ_{19}. The statistical significance in the regression includes: [*]: $p < 0.05$, [**]: $p < 0.01$. PFPeA is excluded due to a small sample size ($n < 3$).

regression between OC and K_d values (for 10 different soils). Their data indicated a comparable trend for PFCAs and for PFSAs where the correlation between OC and K_d increased up to a certain chain length. They found there was no statistically significant correlation (*p*-value > 0.05) for very long PFCAs (PFUnA) and PFSAs (PFNS, PFDS) (Nguyen et al., 2020). Additional studies have reported a dependency of chain length on sorption where, in general, a longer chain length is attributed to an increase in PFAS hydrophobicity, leading to an increased interaction with soil OC (Campos Pereira et al., 2018; Jeon et al., 2011; Liu et al., 2020; Milinovic et al., 2015; Nguyen et al., 2020; Sörengård et al., 2019). Campos Pereira et al. (2018) also reported a break down in this dependency at a chain length of > C_9. Ellis et al. (2004) used Fluorine-19 nuclear magnetic resonance spectroscopy to analyse the intrinsic property change with perfluorinated chain length for PFCAs and found a change in geometry and an increase in molecular rigidity at a chain length between C_8 to C_{10}. It is plausible that the higher molecular rigidity could lead to steric hindrances for very long-chain PFCAs and thus reduce sorption interaction with OC (Campos Pereira et al., 2018; Nguyen et al., 2020).

In a second data analysis step a SLR was conducted for K_{oc} and the mean grain size was selected to investigate a possible effect of the mineral composition of the soil. The variation in K_{oc} values between size fractions (Table 4) indicated that besides interaction with soil organic matter additional sorption interactions occur due to other soil parameters (Gerstl, 1990). The results of the SLR showed a significant negative correlation between mean grain size and K_{oc} values (Fig. 4). The t-values range from −2.7 (PFPeS

and PFHpA) down to −11.3 (PFHxS) indicating a negative slope of the regression line, and hence a decrease of K_{oc} value with increasing grain size. The results for the SLR using log SSA, log clay [%], log silt [%] as independent parameter show for SSA, silt content and clay content significant positive correlations with K_{oc} values for different chain lengths and head groups (Table S15). It should be noted that K_{oc} values of very long PFCAs (> C_{10}) do not significantly correlate with any independent parameter used in this study.

Previously, the mineral composition of a soil fraction has been connected to its size (Hillel, 2008). Larger size fractions, like gravel and sand tend to have higher amounts of primary silicates especially the mineral quartz, which mainly consists of silica (SiO_2). Tang et al. (2010) showed that for mineral surfaces like silica (SiO_2), which are mostly negatively charged under realistic environmental conditions, PFAS sorption is driven by hydrophobic and electrostatic interactions. Whilst silt particles also mainly consist of these primary minerals, they are often coated with strongly adherent clay due to their larger SSA and this alters their physicochemical attributes. Clay particles show higher SSAs compared to bigger size fractions and the particles are mostly negatively charged, leading to unique sorption behaviour (Hillel, 2008). Furthermore, clay particles can incorporate metaloxides between their silica sheets (Kumari and Mohan, 2021). With decreasing grain size, higher concentrations of secondary minerals (mainly clay minerals) were observed in the sample here through the hydrometer analysis. Knight et al. (2019) predicted K_d values for PFOA using a multi linear regression of soil parameters and a partial least squares
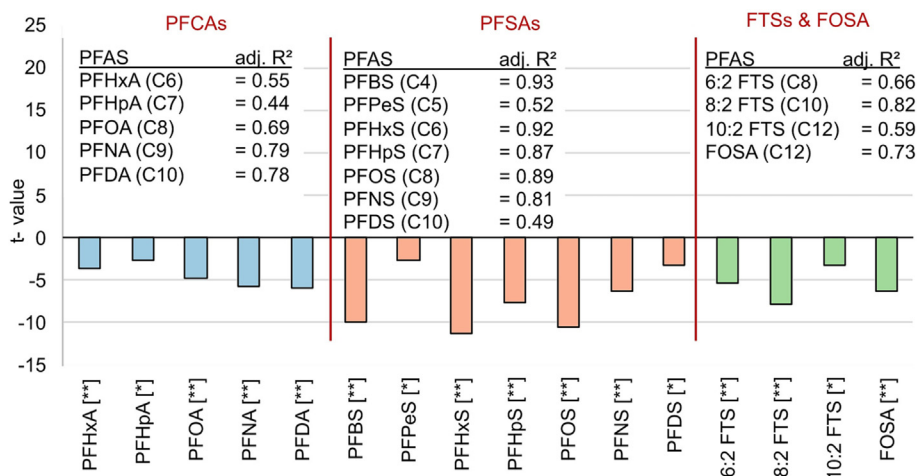

Fig. 4. adj. R^2-values and t-values for the SLR model describing the regression of K_{oc} values with mean grain size. The statistical significance in the regression includes: [*]: $p < 0.05$, [**]: $p < 0.01$. PFUnDA, PFTriDA was excluded as correlations were not significant (p value > 0.05). PFPeA is excluded due to a small sample size (n < 3).

regression using infrared spectra of soil. Their results suggested that the quartz content in the soil was inversely correlated with the sorption of PFAS and positively correlated with silt and clay content. Furthermore, previous studies have shown that sorption to metal oxides via ionic and polar electrostatic interactions contributes to PFAS sorption to soils (Hellsing et al., 2016; Jeon et al., 2011; Tang et al., 2010). Previous studies focusing on clays have reported ionic and polar electrostatic interactions (Jeon et al., 2011), surface complexing and hydrogen-bonding (Zhao et al., 2014) and possibly ligand exchange (Mukhopadhyay et al., 2021) as sorption mechanism for PFAS.

Higher K_{oc} values with decreasing mean grain size found in this study show that PFAS sorption are not exclusively limited to interactions with OC, which is in line with the mentioned studies above. The stronger increase in K_{oc} values between size fractions compared to the derived K_d values (Table S10), indicate that mineral size fractions, as for example secondary minerals (mostly clays) and metalloxides contribute to PFAS sorption through electrostatic dominated sorption mechanisms. This hypothesis is strengthened by the results of the SLR (Table S15), showing negative correlation between mean grain size and positive correlations with clay content, silt content and SSA for K_{oc}.

4. Implications for soil washing

Several European countries have defined thresholds for the reuse of excavated and remediated soil. The Dutch ministry of infrastructure and water management has defined reuse thresholds for soil in residential areas for PFOA (7 µg/kg) and for other individual PFAS (including PFOS at 3 µg/kg) (Ministerie van Infrastructuur en Waterstaat, 2021). In Germany concentrations in leaching water for reused soil (based on batch tests) have been defined for 7 PFAS. For unrestricted reuse the threshold values are ≤ 0.1 ng/mL for PFOS, PFHxS, PFOA, < 6.0 ng/mL for PFHxA, PFBS, < 0.06 ng/mL for PFNA and ≤ 10.0 ng/mL for PFBA (Bieber et al., 2022). One remediation method that has shown promise in reaching low threshold concentrations for coarse-grained as well as fine-grained soils with high clay contents is soil washing (Grimison et al., 2020).

Understanding the partitioning of PFAS between water and different soil size fractions is essential to minimize residual PFAS concentration in processed soil. The results of this study show that coarse-grained fractions and fine-grained fractions must be well separated in the soil washing process to minimize residual PFAS concentrations in soil. The gravel fraction down to the fine sand fraction are the soil fractions which are typically being reused (CDE Group, 2022; Quinnan et al., 2022). Lower K_d values for the sand and the gravel fractions compared to the smaller size fractions indicate that coarser soils are more suitable for soil washing as a remediation technique for PFAS contamination. Fine grained silt and clay fractions are often those that have the highest organic carbon content (OC), and therefore the strongest sorption potential. Longer chain PFAS are those that show increased sorption to OC. To ensure that low enough concentrations are achieved to allow the reuse of this fraction, a large volume of washing water may be needed.

It should also be noted that silt and clay (< 0.063 mm) particles tend to stick to bigger size fractions due to their fine texture. To ensure low residual PFAS concentrations in the sand and gravel fractions it is important to wash these fine materials off. Regarding carbon chain length of PFAS, shorter chain PFAS that have lower K_d values are more easily washed out of soil particles than longer chain PFAS, such as PFOS. It follows that a larger volume of washing water will be needed to achieve the same effect for longer chain PFAS than shorter chain PFAS. In addition, surfactants can be used to enhance the desorption of PFAS from the soil which results in an increased accumulation in the washing water (Bolan et al., 2023). The use of surfactants can therefore increase the efficiency of soil washing especially for finer sized soils which are often characterized by high K_d values. The exceptionally high concentrations found in the SOMR implies that it is crucial to remove this fraction in the soil washing process, potentially through surface skimming.

5. Conclusion

The results of this study supported the hypothesis that PFAS sorption is dependent on grain size, organic carbon content and chain-length of the PFAS. Strong sorption of PFAS to SOMR, which was substantially stronger than any other part of the soil, was reported for the first time. Overall, the K_d values increased with decreasing grain size. For example, the K_d value for PFOS for the silt and clay fraction (< 0.063 mm, 17.1 L/Kg, log K_d 1.23) were approximately 30 times higher compared to the biggest size fraction (gravel, 4 to 8 mm, 0.6 L/Kg, log K_d − 0.25). The highest PFOS K_d value (116.6 L/Kg, log K_d 2.07) was found for the SOMR in the soil. Single linear regression (SLR) indicated that the organic carbon (OC) content in the samples was primarily responsible for sorption. The mineral composition of the size fractions represented by grain size, SSA and silt and clay content also influenced sorption.

With increasingly stringent environmental quality standards regarding PFAS (SCHEER (Scientific Committee on Health, 2022), there will be increasing demand for PFAS remediation. In an ideal situation PFAS contaminated soil could be clean enough to be reused, supporting a circular economy and allowing the reuse of contaminated land and soil. The different concentrations of PFAS found in different size fractions in this study show the importance of understanding the sorption mechanisms that dominate. The clear difference in behaviour of the SOMR in comparison to the other soil fractions is crucial. The uptake of various PFAS and accumulation by plants through pore water uptake was shown in other studies for different crops (Felizeter et al., 2020; Stahl et al., 2009). This mechanism of active root uptake, followed by decay of those roots, could be an explanation for these high concentrations in addition to high OC content, but future work would be needed to investigate this hypothesis. Soil washing results in process water that needs to be cleaned and reused to increase environmental sustainability and economic feasibility of the soil washing process. In this regard standard water treatment techniques like activated carbon filters (Liu et al., 2019; Rodowa et al., 2020) for long-chain PFAS or even more efficient novel treatment trains (Smith et al., 2022; Wanninayake, 2021) can be used to lower PFAS concentrations in water. The soil used in this study contained a considerable amount of silt and clay particles which had a high organic matter content. This means that separating colloidal soil particles from the washing water is important so that PFAS sorbed to these fine particles are not reintroduced to the environment or back into the soil washing process. Future studies should focus on coagulation, flocculation, and sedimentation processes to remove colloids and PFAS from the washing water. In addition, management options should be considered for the PFAS that are concentrated into the sludge and filtercake fraction, for later destructive treatment (e.g., thermal treatment) or landfilling.

Data availability

Data will be made available on request.

Declaration of competing interest

The authors declare that they have no known competing financial interests or personal relationships that could have appeared to influence the work reported in this paper.

CRediT authorship contribution statement

Michel Hubert: Writing – original draft, Conceptualization, Investigation, Methodology, Validation.

Hans Peter H. Arp: Writing – reviewing & editing, Conceptualization; Methodology; Formal Analysis; Project Administration, Supervision, Validation, Funding acquisition

Mona C. Hansen: Writing – reviewing & editing, Formal Analysis

Gabriela Castro: Writing – reviewing & editing, Formal Analysis

Thomas Meyn: Writing – reviewing & editing, Supervision

Alexandros G. Asimakopoulos: Writing – reviewing & editing, Formal Analysis

Sarah Hale: Writing – original draft, reviewing & editing, Investigation, Methodology, Supervision, Validation.

Appendix A. Supplementary data

Supplementary data to this article can be found online at https://doi.org/10.1016/j.scitotenv.2023.162668.

References

Ahrens, L., Taniyasu, S., Yeung, L.W.Y., Yamashita, N., Lam, P.K.S., Ebinghaus, R., 2010. Distribution of polyfluoroalkyl compounds in water, suspended particulate matter and sediment from Tokyo Bay, Japan. Chemosphere 79, 266–272. https://doi.org/10.1016/J.CHEMOSPHERE.2010.01.045.

Anderson, R.H., 2021. The case for direct measures of soil-to-groundwater contaminant mass discharge at AFFF-impacted sites. Cite This: Environ. Sci. Technol. 55, 6583. https://doi.org/10.1021/acs.est.1c01543.

Anderson, D.W., Saggar, S., Bettany, J.R., Stewart, J.W.B., 1981. Particle size fractions and their use in studies of soil organic matter: I. The nature and distribution of forms of carbon, nitrogen, and sulfur1. Soil Sci. Soc. Am. J. 45, 767. https://doi.org/10.2136/sssaj1981.03615995004500040018x.

Arthur, E., Tuller, M., Norgaard, T., Moldrup, P., Chen, C., Ur Rehman, H., Weber, P.L., Knadel, M., Wollesen de Jonge, L., 2023. Contribution of organic carbon to the total specific surface area of soils with varying clay mineralogy. Geoderma 430, 116314. https://doi.org/10.1016/j.geoderma.2022.116314.

Asimakopoulos, A.G., Xue, J., de Carvalho, B.P., Iyer, A., Abualnaja, K.O., Yaghmoor, S.S., Kumosani, T.A., Kannan, K., 2016. Urinary biomarkers of exposure to 57 xenobiotics and its association with oxidative stress in a population in Jeddah, Saudi Arabia. Environ. Res. 150, 573–581. https://doi.org/10.1016/j.envres.2015.11.029.

Baduel, C., Paxman, C.J., Mueller, J.F., 2015. Perfluoroalkyl substances in a firefighting training ground (FTG), distribution and potential future release. J. Hazard. Mater. 296, 46–53. https://doi.org/10.1016/j.jhazmat.2015.03.007.

Barzen-Hanson, K.A., Davis, S.E., Kleber, M., Field, J.A., 2017. Sorption of Fluorotelomer Sulfonates, Fluorotelomer Sulfonamido Betaines, and a Fluorotelomer Sulfonamido Amine in National Foam Aqueous Film-Forming Foam to Soil. https://doi.org/10.1021/acs.est.7b03452.

Bieber, A., Biegel-Engler, A., Gierig, M., Keese, K., Klose, A., Maier, U., Raffelsiefen, M., Schroers, S., Straßburger, T., Ungermann, A., Wiedenhöft, C., 2022. Guidelines for PFAS Assessment – Recommendations for the Uniform Nationwide Assessment of Soil and Water Contamination and for the Disposal of Soil Material Containing PFAS Berlin.

Bolan, N., Sarkar, B., Vithanage, M., Singh, G., Tsang, D.C.W., Mukhopadhyay, R., Ramadass, K., Vinu, A., Sun, Y., Ramanayaka, S., Hoang, S.A., Yan, Y., Li, Y., Rinklebe, J., Li, H., Kirkham, M.B., 2021a. Distribution, behaviour, bioavailability and remediation of poly- and per-fluoroalkyl substances (PFAS) in solid biowastes and biowaste-treated soil. Environ. Int. 155, 106600. https://doi.org/10.1016/j.envint.2021.106600.

Bolan, N., Sarkar, B., Yan, Y., Li, Q., Wijesekara, H., Kannan, K., Tsang, D.C.W., Schauerte, M., Bosch, J., Noll, H., Ok, Y.S., Scheckel, K., Kumpiene, J., Gobindlal, K., Kah, M., Sperry, J., Kirkham, M.B., Wang, H., Tsang, Y.F., Hou, D., Rinklebe, J., 2021b. Remediation of poly- and perfluoroalkyl substances (PFAS) contaminated soils – to mobilize or to immobilize or to degrade? J. Hazard. Mater. 401, 123892. https://doi.org/10.1016/j.jhazmat.2020.123892.

Bolan, S., Padhye, L.P., Mulligan, C.N., Alonso, E.R., Saint-Fort, R., Jasemizad, T., Wang, C., Zhang, T., Rinklebe, J., Wang, H., Siddique, K.H.M., Kirkham, M.B., Bolan, N., 2023. Surfactant-enhanced mobilization of persistent organic pollutants: potential for soil and sediment remediation and unintended consequences. J. Hazard. Mater. 443, 130189. https://doi.org/10.1016/j.jhazmat.2022.130189.

Bräunig, J., Baduel, C., Barnes, C.M., Mueller, J.F., 2019. Leaching and bioavailability of selected perfluoroalkyl acids (PFAAs) from soil contaminated by firefighting activities. Sci. Total Environ. 646, 471–479. https://doi.org/10.1016/j.scitotenv.2018.07.231.

Brusseau, M.L., 2018. Assessing the potential contributions of additional retention processes to PFAS retardation in the subsurface. Sci. Total Environ. 613–614, 176–185. https://doi.org/10.1016/J.SCITOTENV.2017.09.065.

Brusseau, M.L., Anderson, R.H., Guo, B., 2020. PFAS concentrations in soils: background levels versus contaminated sites. Sci. Total Environ. 740, 140017. https://doi.org/10.1016/J.SCITOTENV.2020.140017.

Campos Pereira, H., Ullberg, M., Kleja, D.B., Gustafsson, J.P., Ahrens, L., 2018. Sorption of perfluoroalkyl substances (PFASs) to an organic soil horizon – effect of cation composition and pH. Chemosphere 207, 183–191. https://doi.org/10.1016/J.CHEMOSPHERE.2018.05.012.

Campos-Pereira, H., Kleja, D.B., Sjö, C., Ahrens, L., Klysubun, W., Gustafsson, J.P., 2020. The adsorption of per-and polyfluoroalkyl substances (PFASs) onto ferrihydrite is governed by surface charge. Cite This: Environ. Sci. Technol. 54. https://doi.org/10.1021/acs.est.0c01646.

Castro, G., Fourie, A.J., Marlin, D., Venkatraman, V., González, S.v., Asimakopoulos, A.G., 2022. Occurrence of bisphenols and benzophenone UV filters in wild brown mussels (Perna perna) from Algoa Bay in South Africa. Sci. Total Environ. 813, 152571. https://doi.org/10.1016/j.scitotenv.2021.152571.

CDE Group, 2022. AF DECOM indoor C&D waste recycling wash plant in Norway [WWW Document]. URL https://www.cdegroup.com/about/case-studies/af-decom-norway (accessed 10.24.22).

De Jong, E., 1999. Comparison of three methods of measuring surface area of soils. Can. J. Soil Sci. 79, 345–351. https://doi.org/10.4141/S98-069.

Ellis, D.A., Denkenberger, K.A., Burrow, T.E., Mabury, S.A., 2004. The use of 19 F NMR to interpret the structural properties of perfluorocarboxylate acids: a possible correlation with their environmental disposition. J. Phys. Chem. A 108, 10099–10106. https://doi.org/10.1021/jp049372a.

EN (European Committee for Standardization), 2002. EN 12457-1:2002: Characterisation of waste - Leaching - Compliance test for leaching of granular waste materials and sludges - Part 1: One stage batch test at a liquid to solid ratio of 2 l/kg for materials with high solid content and with particle size below 4 mm (without or with size reduction).

Felizeter, S., Jürling, H., Kotthoff, M., de Voogt, P., McLachlan, M.S., 2020. Influence of soil on the uptake of perfluoroalkyl acids by lettuce: a comparison between a hydroponic study and a field study. Chemosphere 260, 127608. https://doi.org/10.1016/J.CHEMOSPHERE.2020.127608.

Gallen, C., Drage, D., Eaglesham, G., Grant, S., Bowman, M., Mueller, J.F., 2017. Australiawide assessment of perfluoroalkyl substances (PFASs) in landfill leachates. J. Hazard. Mater. 331, 132–141. https://doi.org/10.1016/j.jhazmat.2017.02.006.

Gerstl, Z., 1990. Estimation of organic chemical sorption by soils. J. Contam. Hydrol. 6 (4), 357–375. https://doi.org/10.1016/0169-7722(90)90034-E.

Goldenman, G., Fernandes, M., Holland, M., Tugran, T., Nordin, A., Schoumacher, C., McNeill, A., 2019. The Cost of Inaction. Nordic Council of Ministers, Copenhagen https://doi.org/10.6027/TN2019-516.

Grimison, C., Brookman, I., Hunt, J., Lucas, J., 2020. Ventia Submission - PFAS Subcommittee of the Joint Standing Committee in Foreign Affairs, Defence and Trade - Remediation of PFAS-related impacts – ongoing scrutiny and review.

Grimison, C., Knight, E.R., Nguyen, T.M.H., Nagle, N., Kabiri, S., Bräunig, J., Navarro, D.A., Kookana, R.S., Higgins, C.P., McLaughlin, M.J., Mueller, J.F., 2023. The efficacy of soil washing for the remediation of per- and poly-fluoroalkyl substances (PFASs) in the field. J. Hazard. Mater. 445, 130441. https://doi.org/10.1016/j.jhazmat.2022.130441.

Hale, S.E., Arp, H.P.H., Slinde, G.A., Wade, E.J., Bjørseth, K., Breedveld, G.D., Straith, B.F., Moe, K.G., Jartun, M., Høisæter, Å., 2017. Sorbent amendment as a remediation strategy to reduce PFAS mobility and leaching in a contaminated sandy soil from a Norwegian firefighting training facility. Chemosphere 171, 9–18. https://doi.org/10.1016/J.CHEMOSPHERE.2016.12.057.

Hellsing, M.S., Josefsson, S., Hughes, A.v., Ahrens, L., 2016. Sorption of perfluoroalkyl substances to two types of minerals. Chemosphere 159, 385–391. https://doi.org/10.1016/J.CHEMOSPHERE.2016.06.016.

Helsel, D.R., 2006. Fabricating data: how substituting values for nondetects can ruin results, and what can be done about it. Chemosphere 65, 2434–2439. https://doi.org/10.1016/J.CHEMOSPHERE.2006.04.051.

Higgins, C., Richard, L., 2006. Sorption of Perfluorinated Surfactants on Sediments †. https://doi.org/10.1021/es061000n.

Hillel, D., 2008. Soil physical attributes. Soil in the Environment, pp. 55–77 https://doi.org/10.1016/B978-0-12-348536-6.50010-1.

Høisæter, Å., Breedveld, G.D., 2022. Leaching potential of per- and polyfluoroalkyl substances from source zones with historic contamination of aqueous film forming foam - a surfactant mixture problem. Environ. Adv. 8, 100222. https://doi.org/10.1016/j.envadv.2022.100222.

Høisæter, Å., Aasen, G., Haug, G., 2015. Aktuelle tiltake i imetta sone ved brannøvingsfeltet på Oslo Lufthavn, Gardermoen Oslo.

Høisæter, Å., Pfaff, A., Breedveld, G.D., 2019. Leaching and transport of PFAS from aqueous film-forming foam (AFFF) in the unsaturated soil at a firefighting training facility under cold climatic conditions. J. Contam. Hydrol. 222, 112–122. https://doi.org/10.1016/J.JCONHYD.2019.02.010.

Høisæter, Å., Arp, H.P.H., Slinde, G., Knutsen, H., Hale, S.E., Breedveld, G.D., Hansen, M.C., 2021. Excavated vs novel in situ soil washing as a remediation strategy for sandy soils impacted with per- and polyfluoroalkyl substances from aqueous film forming foams. Sci. Total Environ. 794, 148763. https://doi.org/10.1016/j.scitotenv.2021.148763.

Houtz, E.F., Higgins, C.P., Field, J.A., Sedlak, D.L., 2013. Persistence of Perfluoroalkyl Acid Precursors in AFFF-Impacted Groundwater and Soil. https://doi.org/10.1021/es4018877.

Huang, D., Khan, N.A., Wang, G., Carroll, K.C., Brusseau, M.L., 2022. The co-transport of PFAS and Cr(VI) in porous media. Chemosphere 286, 131834. https://doi.org/10.1016/J.CHEMOSPHERE.2021.131834.

ISO (International Organization for standardization), 2016. ISO 17892-4:2016 - Geotechnical investigation and testing - Laboratory testing of soil - Part 4: Determination of particle size distribution.

Jeon, J., Kannan, K., Lim, B.J., An, K.G., Kim, S.D., 2011. Effects of salinity and organic matter on the partitioning of perfluoroalkyl acid (PFAs) to clay particles. J. Environ. Monit. 13, 1803. https://doi.org/10.1039/c0em00791a.

Kaiser, K., Guggenberger, G., Zech, W., 1996. Sorption of DOM and DOM fractions to forest soils. Geoderma 74, 281–303. https://doi.org/10.1016/S0016-7061(96)00071-7.

Knight, E.R., Janik, L.J., Navarro, D.A., Kookana, R.S., McLaughlin, M.J., 2019. Predicting partitioning of radiolabelled 14C-PFOA in a range of soils using diffuse reflectance infrared spectroscopy. Sci. Total Environ. 686, 505–513. https://doi.org/10.1016/J.SCITOTENV.2019.05.339.

Kookana, R.S., Navarro, D.A., Kabiri, S., McLaughlin, M.J., 2022. Key properties governing sorption–desorption behaviour of poly- and perfluoroalkyl substances in saturated and unsaturated soils: a review. Soil Res. https://doi.org/10.1071/SR22183.

Kumari, N., Mohan, C., 2021. Basics of clay minerals and their characteristic properties. Clay and Clay Minerals. IntechOpen https://doi.org/10.5772/intechopen.97672.

Kurwadkar, S., Dane, J., Kanel, S.R., Nadagouda, M.N., Cawdrey, R.W., Ambade, B., Struckhoff, G.C., Wilkin, R., 2022. Per- and polyfluoroalkyl substances in water and wastewater: a critical review of their global occurrence and distribution. Sci. Total Environ. 809, 151003. https://doi.org/10.1016/j.scitotenv.2021.151003.

Langberg, H.A., Breedveld, G.D., Grønning, H.M., Kvennås, M., Jenssen, B.M., Hale, S.E., 2019. Bioaccumulation of fluorotelomer sulfonates and perfluoroalkyl acids in marine organisms living in aqueous film-forming foam impacted waters. Environ. Sci. Technol. 53, 10951–10960. https://doi.org/10.1021/acs.est.9b00927.

Lath, S., Knight, E.R., Navarro, D.A., Kookana, R.S., McLaughlin, M.J., 2019. Sorption of PFOA onto different laboratory materials: filter membranes and centrifuge tubes. Chemosphere 222, 671–678. https://doi.org/10.1016/J.CHEMOSPHERE.2019.01.096.

Li, Y., Oliver, D.P., Kookana, R.S., 2018. A critical analysis of published data to discern the role of soil and sediment properties in determining sorption of per and polyfluoroalkyl substances (PFASs). Sci. Total Environ. 628–629, 110–120. https://doi.org/10.1016/J.SCITOTENV.2018.01.167.

Liu, C.J., Werner, D., Bellona, C., 2019. Removal of per- and polyfluoroalkyl substances (PFASs) from contaminated groundwater using granular activated carbon: a pilot-scale study with breakthrough modeling. Environ. Sci. (Camb.) 5, 1844–1853. https://doi.org/10.1039/C9EW00349E.

Liu, Y., Qi, F., Fang, C., Naidu, R., Duan, L., Dharmarajan, R., Annamalai, P., 2020. The effects of soil properties and co-contaminants on sorption of perfluorooctane sulfonate (PFOS) in contrasting soils. Environ. Technol. Innov. 19, 100965. https://doi.org/10.1016/J.ETI.2020.100965.

Maizel, A., Shea, S., Nickerson, A., Schaefer, C., Higgins, C.P., 2021. Release of per- and polyfluoroalkyl substances from aqueous film-forming foam impacted soils. Environ. Sci. Technol. 55, 14617–14627. https://doi.org/10.1021/acs.est.1c02871.

Masoner, J.R., Kolpin, D.W., Cozzarelli, I.M., Smalling, K.L., Bolyard, S.C., Field, J.A., Furlong, E.T., Gray, J.L., Lozinski, D., Reinhart, D., Rodowa, A., Bradley, P.M., 2020. Landfill leachate contributes per-/poly-fluoroalkyl substances (PFAS) and pharmaceuticals to municipal wastewater †. Cite this: Environ. Sci.: Water Res. Technol. 6, 1300. https://doi.org/10.1039/d0ew00045k.

McMahon, P.B., Tokranov, A.K., Bexfield, L.M., Lindsey, B.D., Johnson, T.D., Lombard, M.A., Watson, E., 2022. Perfluoroalkyl and polyfluoroalkyl substances in groundwater used as a source of drinking water in the eastern United States. Environ. Sci. Technol. 56, 2279–2288. https://doi.org/10.1021/acs.est.1c04795.

Mei, W., Sun, H., Song, M., Jiang, L., Li, Y., Lu, W., Ying, G.G., Luo, C., Zhang, G., 2021. Per- and polyfluoroalkyl substances (PFASs) in the soil–plant system: sorption, root uptake, and translocation. Environ. Int. 156, 106642. https://doi.org/10.1016/J.ENVINT.2021.106642.

Mejia-Avendañ, S., Zhi, Y., Yan, B., Liu, J., 2020. Sorption of polyfluoroalkyl surfactants on surface soils: effect of molecular structures, soil properties, and solution chemistry. Cite This: Environ. Sci. Technol. 54, 1513–1521. https://doi.org/10.1021/acs.est.9b04989.

Milinovic, J., Lacorte, S., Vidal, M., Rigol, A., 2015. Sorption behaviour of perfluoroalkyl substances in soils. Sci. Total Environ. 511, 63–71. https://doi.org/10.1016/J.SCITOTENV.2014.12.017.

Ministerie van Infrastructuur en Waterstaat, 2021. Handelingskader voor hergebruik van PFAS-houdende grond en baggerspecie (versie december 2021).

Mukhopadhyay, R., Sarkar, B., Palansooriya, K.N., Dar, J.Y., Bolan, N.S., Parikh, S.J., Sonne, C., Ok, Y.S., 2021. Natural and engineered clays and clay minerals for the removal of poly- and perfluoroalkyl substances from water: state-of-the-art and future perspectives. Adv. Colloid Interf. Sci. 297, 102537. https://doi.org/10.1016/j.cis.2021.102537.

Nguyen, T.M.H., Brä, J., Thompson, K., Thompson, J., Kabiri, S., Navarro, D.A., Kookana, R.S., Grimison, C., Barnes, C.M., Higgins, C.P., Mclaughlin, M.J., Mueller, J.F., 2020. Influences of chemical properties, soil properties, and solution pH on soil−water partitioning coefficients of per-and polyfluoroalkyl substances (PFASs). Cite This: Environ. Sci. Technol. 54, 15883–15892. https://doi.org/10.1021/acs.est.0c05705.

Nickerson, A., Maizel, A.C., Kulkarni, P.R., Adamson, D.T., Kornuc, J.J., Higgins, C.P., 2020. Enhanced extraction of AFFF-associated PFASs from source zone soils. Environ. Sci. Technol. 54, 4952–4962. https://doi.org/10.1021/acs.est.0c00792.

Niskanen, R., Mänthylahti, V., 1988. Determination of soil specific surface area by water vapour adsorption III - comparison of surface areas determined by water vapor and nitrogen gas adsorption. Agric. Food Sci. 60, 73–79. https://doi.org/10.23986/afsci.72277.

O'Connor, J., Bolan, N.S., Kumar, M., Nitai, A.S., Ahmed, M.B., Bolan, S.S., Vithanage, M., Rinklebe, J., Mukhopadhyay, R., Srivastava, P., Sarkar, B., Bhatnagar, A., Wang, H., Siddique, K.H.M., Kirkham, M.B., 2022. Distribution, transformation and remediation of poly- and per-fluoroalkyl substances (PFAS) in wastewater sources. Process Saf. Environ. Prot. 164, 91–108. https://doi.org/10.1016/j.psep.2022.06.002.

OECD, 2001. Test No. 121: Estimation of the Adsorption Coefficient (Koc) on Soil and on Sewage Sludge using High Performance Liquid Chromatography (HPLC). OECD https://doi.org/10.1787/9789264069909-en.

OECD, 2011. Portal on Per and Poly Fluorinated Chemicals - About PFAS [WWW Document]. URL (accessed 10.10.22) https://www.oecd.org/chemicalsafety/portal-perfluorinated-chemicals/aboutpfass/.

Pennell, K.D., Abriola, L.M., Boyd, S.A., 1995. Surface area of soil organic matter reexamined. Soil Sci. Soc. Am. J. 59, 1012–1018. https://doi.org/10.2136/sssaj1995.03615995005900040008x.

Pignatello, J.J., Kwon, S., Lu, Y., 2006. Effect of natural organic substances on the surface and adsorptive properties of environmental black carbon (Char): attenuation of surface activity by humic and fulvic acids. Environ Sci Technol 40, 7757–7763. https://doi.org/10.1021/es061307m.

Quinnan, J., Morrell, C., Nagle, Nathan, Maynard, K.G., 2022. Ex Situ Soil Washing to Remove PFAS Adsorbed to Soils From Source Zones. https://doi.org/10.1002/rem.21727.

Raposo, F., Barceló, D., 2021. Challenges and strategies of matrix effects using chromatography-mass spectrometry: an overview from research versus regulatory viewpoints. TrAC Trends Anal. Chem. 134, 116068. https://doi.org/10.1016/j.trac.2020.116068.

Rayne, S., Forest, K., 2009. Comment on "Indirect photolysis of perfluorochemicals: hydroxyl radical-initiated oxidation of N-ethyl perfluorooctane sulfonamido acetate (N-EtFOSAA) and other perfluoroalkanesulfonamides". Environ Sci Technol 43, 7995–7996. https://doi.org/10.1021/es9022464.

Rodowa, A.E., Knappe, D.R.U., Chiang, S.-Y.D., Pohlmann, D., Varley, C., Bodour, A., Field, J.A., 2020. Pilot scale removal of per- and polyfluoroalkyl substances and precursors from AFFF-impacted groundwater by granular activated carbon. Environ. Sci. (Camb.) 6, 1083–1094. https://doi.org/10.1039/C9EW00936A.

Ross, I., McDonough, J., Miles, J., Storch, P., Thelakkat Kochunarayanan, P., Kalve, E., Hurst, J., Dasgupta, S., Burdick, J., 2018. A review of emerging technologies for remediation of PFASs. Remediat. J. 28, 101–126. https://doi.org/10.1002/rem.21553.

Schaefer, C.E., Nguyen, D., Christie, E., Shea, S., Higgins, C.P., Field, J.A., 2021. Desorption of poly- and perfluoroalkyl substances from soil historically impacted with aqueous film-forming foam. J. Environ. Eng. 147. https://doi.org/10.1061/(ASCE)EE.1943-7870.0001846.

SCHEER (Scientific Committee on Health, Environmental and Emerging Riskscollab, 2022. Final Opinion on Draft Environmental Quality Standards for Priority Substances under the Water Framework Directive - PFAS.

Smith, S.J., Wiberg, K., Mccleaf, P., Ahrens, L., 2022. Pilot-Scale Continuous Foam Fractionation for the Removal of Per-and Polyfluoroalkyl Substances (PFAS) from Landfill Leachate. https://doi.org/10.1021/acsestwater.2c00063.

Sokołowska, Z., 2011. Specific surface area of soils and plants. In: Gliński, J., Horabik, J., Lipiec, J. (Eds.), Encyclopedia of Agrophysics. Springer, Dordrecht, pp. 839–844 https://doi.org/10.1007/978-90-481-3585-1_265.

Sörengård, M., Kleja, D.B., Ahrens, L., 2019. Stabilization and solidification remediation of soil contaminated with poly- and perfluoroalkyl substances (PFASs). J. Hazard. Mater. 367, 639–646. https://doi.org/10.1016/J.JHAZMAT.2019.01.005.

Sörengård, M., Franke, V., Tröger, R., Ahrens, L., 2020. Losses of poly- and perfluoroalkyl substances to syringe filter materials. J. Chromatogr. A 1609, 460430. https://doi.org/10.1016/J.CHROMA.2019.460430.

Sörengård, M., Bergström, S., McCleaf, P., Wiberg, K., Ahrens, L., 2022. Long-distance transport of per- and polyfluoroalkyl substances (PFAS) in a Swedish drinking water aquifer. Environ. Pollut. 311, 119981. https://doi.org/10.1016/J.ENVPOL.2022.119981.

Stahl, T., Heyn, A.J., Thiele, A.H., Hüther, A.J., Failing, A.K., Georgii, A.S., Brunn, A.H., Heyn, J., Hüther, J., Failing, K., Brunn, H., 2009. Carryover of perfluorooctanoic acid (PFOA) and perfluorooctane sulfonate (PFOS) from soil to plants. Arch. Environ. Contam. Toxicol. 57, 289–298. https://doi.org/10.1007/s00244-008-9272-9.

Tang, C.Y., Shiang Fu, Q., Gao, D., Criddle, C.S., Leckie, J.O., 2010. Effect of solution chemistry on the adsorption of perfluorooctane sulfonate onto mineral surfaces. Water Res. 44, 2654–2662. https://doi.org/10.1016/J.WATRES.2010.01.038.

The Commission of the European Communities, 2009. Amending Regulation (EC) No 1907/2006 of the European Parliament and of the Council on the Registration, Evaluation, Authorisation and Restriction of Chemicals (REACH) as regards Annex XVII. Off. J. Eur. Union 569 COMMISSION REGULATION (EC) No 552/2009. Document 02006R1907-20221217.

Umeh, A.C., Naidu, R., Shilpi, S., Boateng, E.B., Rahman, A., Cousins, I.T., Chadalavada, S., Lamb, D., Bowman, M., 2021. Sorption of PFOS in 114 well-characterized tropical and temperate soils: application of multivariate and artificial neural network analyses. Cite This: Environ. Sci. Technol. 55, 1779–1789. https://doi.org/10.1021/acs.est.0c07202.

Wang, Qingren, Li, Yuncong, Wang, Y., Wang, Q., Li, Y., Li, Y., 2011. Optimizing the weight loss-on-ignition methodology to quantify organic and carbonate carbon of sediments from diverse sources. Environ. Monit. Assess. 174, 241–257. https://doi.org/10.1007/s10661-010-1454-z.

Wang, C., Yan, B., Munoz, G., Sauvé, S., Liu, J., 2021. Modified clays reduce leaching of per- and polyfluoroalkyl substances from AFFF contaminated soils. AWWA Water Sci. 3. https://doi.org/10.1002/aws2.1241.

Wanninayake, D.M., 2021. Comparison of currently available PFAS remediation technologies in water: a review. J. Environ. Manag. 283, 111977. https://doi.org/10.1016/J.JENVMAN.2021.111977.

Xiao, F., Jin, B., Golovko, S.A., Golovko, M.Y., Xing, B., 2019. Sorption and desorption mechanisms of cationic and zwitterionic per- and polyfluoroalkyl substances in natural soils: thermodynamics and hysteresis. Environ. Sci. Technol. 53, 11818–11827. https://doi.org/10.1021/acs.est.9b05379.

Yang, X.M., Drury, C.F., Reynolds, W.D., Yang, J.Y., 2016. How do changes in bulk soil organic carbon content affect carbon concentrations in individual soil particle fractions? Sci. Rep. 6, 27173. https://doi.org/10.1038/srep27173.

Yukselen, Y., Kaya, A., 2006. Comparison of methods for determining specific surface area of soils. J. Geotech. Geoenviron. 132, 931–936. https://doi.org/10.1061/(ASCE)1090-0241(2006)132:7(931).

Zareitalabad, P., Siemens, J., Hamer, M., Amelung, W., 2013. Perfluorooctanoic acid (PFOA) and perfluorooctanesulfonic acid (PFOS) in surface waters, sediments, soils and wastewater – a review on concentrations and distribution coefficients. Chemosphere 91, 725–732. https://doi.org/10.1016/j.chemosphere.2013.02.024.

Zhang, C., Yan, H., Li, F., Hu, X., Zhou, Q., 2013. Sorption of short- and long-chain perfluoroalkyl surfactants on sewage sludges. J. Hazard. Mater. 260, 689–699. https://doi.org/10.1016/J.JHAZMAT.2013.06.022.

Zhao, L., Bian, J., Zhang, Y., Zhu, L., Liu, Z., 2014. Comparison of the sorption behaviors and mechanisms of perfluorosulfonates and perfluorocarboxylic acids on three kinds of clay minerals. Chemosphere 114, 51–58. https://doi.org/10.1016/J.CHEMOSPHERE.2014.03.098.

Zhu, X., Song, X., Schwarzbauer, J., 2021. First insights into the formation and long-term dynamic behaviors of nonextractable perfluorooctanesulfonate and its alternative 6:2 chlorinated polyfluorinated ether sulfonate residues in a silty clay soil. Sci. Total Environ. 761, 143230. https://doi.org/10.1016/j.scitotenv.2020.143230.